Leaching Kinetics of Praseodymium in Sulfuric Acid of Rare Earth Elements (REE) Slag Concentrated by Pyrometallurgy from Magnetite Ore

Chul-Joo Kim*, Ho-Sung Yoon*, Kyung Woo Chung*, Jin-Young Lee*, Sung-Don Kim*, Shun Myung Shin*,
Hyung-Seop Kim**, Jong-Tae Cho**, Ji-Hye Kim**, Eun-Ji Lee**, Se-Il Lee** and Seung-Joon Yoo**,†

*Korea Institute of Geoscience and Mineral Resources, 124 Gwahang-no, Yuseong-gu, Daejeon 305-350, Korea
**Department of Environmental and Chemical Engineering, Seonam University, 7-111 Pyeongchon-gil, Songak, Asan 336-922, Korea
(Received 25 June 2014; Received in revised form 20 July 2014; accepted 23 July 2014)

Abstract – A leaching kinetics was conducted for the purpose of recovery of praseodymium in sulfuric acid (H_2SO_4) from REE slag concentrated by the smelting reduction process in an arc furnace as a reactant. The concentration of H_2SO_4 was fixed at an excess ratio under the condition of slurry density of 1.500 g slag/L, 0.3 mol H_2SO_4, and the effect of temperatures was investigated under the condition of 30 to 80 ℃. As a result, praseodymium oxide (Pr_6O_{11}) existing in the slag was completely converted into praseodymium sulfate ($Pr_2(SO_4)_3 \cdot 8H_2O$) after the leaching of 5 h. On the basis of the shrinking core model with a shape of sphere, the first leaching reaction was determined by chemical reaction mechanism. Generally, the solubility of pure REEs decreases with the increase of leaching temperatures in sulfuric acid, but REE slag was oppositely increased with increasing temperatures. It occurs because the ash layer included in the slag is affected as a resistance against the leaching. By using the Arrhenius expression, the apparent activation energy of the first chemical reaction was determined to be 9.195 kJmol^{-1}. In the second stage, the leaching rate is determined by the ash layer diffusion mechanism. The apparent activation energy of the second ash layer diffusion was determined to be 19.106 kJmol^{-1}. These relative low activation energy values were obtained by the existence of unreacted ash layer in the REE slag.

Key words: Leaching, REE Slag, Shrinking Core Model, Praseodymium Oxide, Praseodymium Sulfate, Sulfuric Acid

1. Introduction

REEs (rare earth elements), according to the IUPAC definition, is a group of chemical elements with lanthanides plus scandium and yttrium. Based on their location in the periodic table and their atomic weights, it is possible to classify these elements into light REEs or LREEs (lanthanum, cerium, praseodymium, neodymium, promethium and samarium, with atomic numbers 57-62) and heavy REEs or HREEs (europium, gadolinium, terbium, dysprosium, holmium, erbium, thulium, ytterbium, lutetium atomic number 63-71) [1]. The lanthanides among the REEs are the filling of the 4f outer-shell electrons. The electronic structure of the lanthanide elements has $[Xe]5d^1 6s^2 4f^n$ with minor exceptions. These 4f orbitals are buried inside atom and are shielded from the atom's environment by the 4d and 5p electrons. The 4f orbitals in the lanthanides are sufficiently low in energy that the electrons are seldom ionized or shared [2,3].

REEs are broadly used to the high-tech industry like high strength permanent magnets, lasers, automotive catalytic converters, fiber optics/superconductors, and electronic devices. Because of the ongoing development of new advanced technologies, an ever-increasing demand on REEs will persist in the international markets. China dominates the world market of REEs with over 95% recently [4].

The demand for REE metals has rapidly been increasing, but China has steadily increased export taxes on REEs and has nationally been restricting the export quotas of them. Therefore, REE resources-free countries, such as South Korea and Japan, have to develop the new raw material resources like low-grade REE sources. It is well-known that hydrometallurgy is the most effective method for the leaching of low-grade raw materials because of the selective leaching by solvent, low process cost and occurrence of relatively small pollutants [5-17].

This study was also conducted to recover REE metals from low-grade monazite-type REE raw material and selected praseodymium as a research objective among the components in REE slag because praseodymium cost increased as highest growth rate of price from 14 US$/kg to now 175 US$/kg recently [4].

The leaching mechanism of slag was hypothesized by a shrinking core model with a constant size and a two-stage model with a chemical reaction and ash layer diffusion because some part of the REE slag was partly oxidized by arc furnace even though it is reduced through the smelting reduction process. Finally, the REE slag remains in the ash layers after the completion of leaching as shown in Fig. 1.

1-1. Surface reaction control
Assuming the first-order chemical reaction rate model based on the shrinking core model with the same particle size before and after
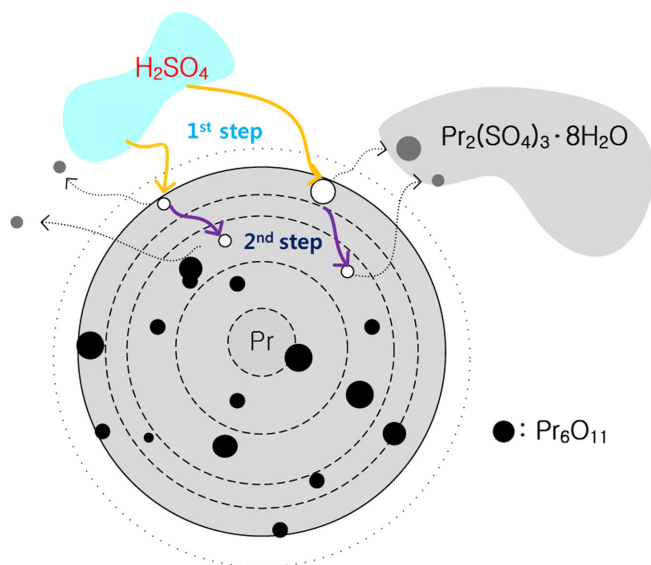
Fig. 1. Schematic diagram for leaching behavior of reacting REE slag particles.

the leaching [18,19] that has a shape of a spherical particle, the chemical reaction may be expressed in the following Eq. (2).

$$-\frac{1}{S_{ex}}\frac{dN_B}{dt} = -\frac{\rho_B}{S_{ex}} \cdot S_{ex} \cdot \frac{dr_c}{dt} = -\rho_B \cdot \frac{dr_c}{dt} = \frac{1}{3}k_s C_A \qquad (2)$$

However, the variation of C_A can be neglected during the chemical reaction because the H_2SO_4 is added into the reactor more excessively than the stoichiometric ratio.

Since C_A can be accepted as a constant in Eq. (2), this model is modified as follows:

$$-\rho_B \cdot \int_R^{r_c} dr_c = \frac{1}{3}k_s C_{A0}(1-X_A)t \qquad (3)$$

$$\frac{3\rho_B R}{k_s}\left[1-\left(\frac{r_c}{R}\right)\right] = C_{A0}(1-X_A)t \qquad (4)$$

This can be written in terms of fractional conversion by noting that

$$1-X_B = \frac{\frac{4}{3}\pi r_c^3}{\frac{4}{3}\pi R^3} = \left(\frac{r_c}{R}\right)^3$$

Therefore

$$\left(\frac{r_c}{R}\right) = (1-X_B)^{1/3}$$

$$1-(1-X_B)^{1/3} = k_{c,chem}t \qquad (5)$$

The variation of H_2SO_4 (X_A) can be neglected because it is added excessively.

$k_{c,chem}$ is the apparent rate constant for chemical reaction and inverse of the time required for complete conversion is given when $r_c = 0$.

$$k_{c,chem} = \frac{C_{A0}k_s}{3\rho_B R} \qquad (6)$$

1-2. Ash layer diffusion control

During the chemical reaction, the praseodymium component on the surface of REE slag is first leached out. Then the ash layers remaining after the initial chemical reaction become thicker and act as a resistance for H_2SO_4 solution to go inner from the surface. Therefore, the ash layer diffusion can be considered as a second step for the rate determining stage. In diffusion controlled reaction models, there are many kinetic equations [20,21]. The reaction rate can be expressed in terms of the diffusion rate of H_2SO_4 through the ash layers as follows:

$$1-3(1-X_B)^{2/3}+2(1-X_B) = k_{c,ash}t \qquad (7)$$

where $k_{c,ash}$ is the apparent rate constant for ash layer diffusion and inverse of the time required for complete conversion of a particle, $r_c = 0$.

$$k_{c,ash} = \frac{2D_e C_{A0}}{\rho_B R^2} \qquad (8)$$

2. Materials and Methods

The raw material was mined from Hongcheongun in Korea and concentrated by the smelting reduction process in an arc furnace. The REE slag obtained after the smelting reduction process was milled and washed with water to remove impurities on the REE slag. Finally, particle size had a size range of 100 to 200 μm.

The concentrations of H_2SO_4 were added into reactor as the excess ratios of 0.1 to 0.3 M over the stoichiometric ratio, but the leaching rate was not significantly affected by the excess ratio of H_2SO_4 concentration. Nevertheless, the H_2SO_4 concentration was fixed at 0.3 M higher than the stoichiometric ratio in this experiment for the concentration of H_2SO_4 to be constant during reaction. Accordingly, the concentration of H_2SO_4 was assumed to be constant. All the solutions indicated the scale of pH 1.0.

3. Analysis

Metal compositions included in the REE slag were analyzed under the condition of 1,300 W RF Power, 27.12 MHz RF frequency, 13 L/min Coolant gas flow and 0.9 L/min Nebulizer gas flow by inductively coupled plasma-mass spectrometry (ICP-MS, X-series (X5), Thermo Elemental, UK). ICP-MS was found to be the most suitable technique for the determination of REE content because it exhibits high sensitivity and accuracy, with high sample throughput. ICP-MS also allows rapid simultaneous multi-element determination [22].
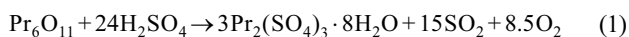
The crystal structure and crystallinity of the REE slag were analyzed under the following analytical conditions (CuKα source, scanning speed 1°/min, 40 kV, 40 mA, 0°≤2θ≤90° scanning range) by X-ray diffraction spectroscopy (D8 ADVANCE, BRUKER AXS).

The pH values were measured by pH electrode in Advanced Electrochemistry Meter [Orion VERSASTAR, Thermo Scientific].

Praseodymium ion concentration was analyzed by inductively cou-pled plasma-atomic emission spectrometry (ICP-AES, *i*CAP6000, Thermo Fisher, UK) during the leaching. When viscous silicate solu-tion is injected into the plasma and nebulizer is blocked, the accuracy and detection limits of the ICP-AES are usually degraded. This problem can be avoided by limiting the input of viscous solution and frequent washing of the nebulizer.

4. Results and Discussion

Pr_6O_{11} existing in the REE slag is converted into $Pr_2(SO_4)_3$ phase under H_2SO_4 solution as in the following eq. (1). The reaction has a stoichiometric ratio of 3 mol H_2SO_4 per 1 mol Pr_6O_{11}. As shown in Eh-pH diagram of Fig. 2, Pr_6O_{11} is reduced into $Pr_2(SO_4)_3$ under the condition below pH 9.8 and is precipitated by $Pr(OH)_3$ over the pH. Accordingly, the leaching is desirable to keep below the pH 9.8 for the sake of efficient leaching of praseodymium.

$$Pr_6O_{11} + 24H_2SO_4 \rightarrow 3Pr_2(SO_4)_3 \cdot 8H_2O + 15SO_2 + 8.5O_2 \quad (1)$$

There are many chemical components in the REE slag [23], and the slag exists as various metal compounds as oxides, phosphates,
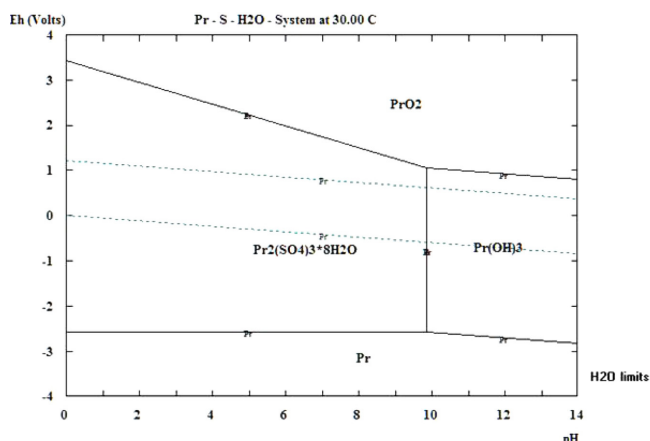

Fig. 2. Eh-pH diagram of Pr chemical species in H_2SO_4 solution.
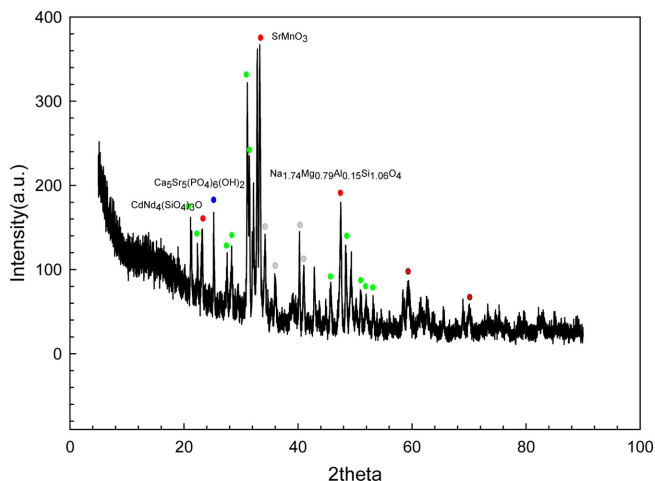

Fig. 3. XRD pattern of REE Slag reactant.

or silicates as shown in Fig. 3 because it is treated under the reduc-tion atmosphere of high temperature [24].

If the metals existing in the slag consist of simple metal oxide forms, they can easily be converted into metal sulfate forms thermo-dynamically as follows; Gibb's free energy was calculated at 30 °C. The following thermodynamic data are about the metal oxides exist-ing more than 0.4% in the REE slag.

At this time, most of the data were taken from HSC 5.11 software database [25].
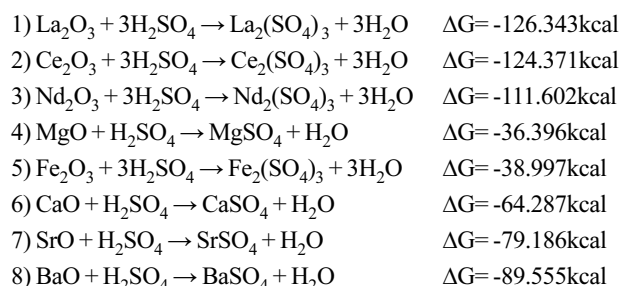
1) $La_2O_3 + 3H_2SO_4 \rightarrow La_2(SO_4)_3 + 3H_2O$ ΔG= -126.343kcal
2) $Ce_2O_3 + 3H_2SO_4 \rightarrow Ce_2(SO_4)_3 + 3H_2O$ ΔG= -124.371kcal
3) $Nd_2O_3 + 3H_2SO_4 \rightarrow Nd_2(SO_4)_3 + 3H_2O$ ΔG= -111.602kcal
4) $MgO + H_2SO_4 \rightarrow MgSO_4 + H_2O$ ΔG= -36.396kcal
5) $Fe_2O_3 + 3H_2SO_4 \rightarrow Fe_2(SO_4)_3 + 3H_2O$ ΔG= -38.997kcal
6) $CaO + H_2SO_4 \rightarrow CaSO_4 + H_2O$ ΔG= -64.287kcal
7) $SrO + H_2SO_4 \rightarrow SrSO_4 + H_2O$ ΔG= -79.186kcal
8) $BaO + H_2SO_4 \rightarrow BaSO_4 + H_2O$ ΔG= -89.555kcal

Table 1 is an elemental composition of REE slag analyzed by ICP-MS. As shown in Table 1, praseodymium component in is included 0.41% in the REE slag. Praseodymium is a LREE (light rare earth element) component to be able to leach in acidic solution next to lanthanum component, cerium and neodymium. Therefore, we selected the praseodymium as a leaching objective.

The leaching experiment was conducted under the condition of a 1.500 g slag/L H_2SO_4, with agitation at a temperature range of 30 to 80 °C. If it is assumed that REE components exist as the forms of the simple metal oxide, the stoichiometric ratio of H_2SO_4 (Merck, 98%) required to be converted into sulfate forms is about 0.0018 mol/L per 1.500 g slag.

Using the pure Pr_6O_{11} reagent (99%, Alfa Aesar, black and dark-green powders), the effect of H_2SO_4 concentrations was investi-gated. A leaching experiment was conducted at two different H_2SO_4 concentrations of a stoichiometric ratio (3 mol H_2SO_4/mol Pr_6O_{11}) and an excess ratio (4 mol H_2SO_4/mol Pr_6O_{11}). As the results, $Pr(OH)_3$ precipitate was not produced at all the two conditions as the shown in Fig. 4. In the experiment of pure Pr_6O_{11} reagent, the final pHs of leached solution were found to 2.991 at the H_2SO_4 concentration of stoichiometric ratio and 1.712 at the excess ratio. As described before, it depends on the final pH whether the solution is $Pr_2(SO_4)_3$ phase or $Pr(OH)_3$ precipitate phase.

Table 1. Elemental composition of REE slag analyzed by ICP-MS

Element	Conc.	Element	Conc.	Element	Conc.
La	2.76%	Tb	23.5 ppm	U	1.8 ppm
Ce	4.60%	Dy	53.6 ppm	Fe	0.7%
Pr	0.41%	Ho	5.4 ppm	Ca	13.9%
Nd	1.14%	Er	16.8 ppm	Mg	7.1%
Sm	830.7 ppm	Tm	0.8ppm	Ba	2.16%
Eu	158.5 ppm	Yb	9.0 ppm	Sr	9.84%
Gd	278.1 ppm	Lu	1.6 ppm	Y	122 ppm

Fig. 4. Pr reached solutions of stoichiometric ratio and excess ratio.

Fig. 5. Photograph of REE slag and REE leached solution.

REE slag is composed of metal oxide, silicate, and ash layers. It has a black color and a size range of 100 to 200 μm. The right side of Fig. 5 shows a leached solution.

Although there was no noticeable change in size of the slag before and after the leaching, the praseodymium content in the slag was completely leached into the solution after the leaching reaction.

$Pr(OH)_3$ precipitate was never produced at the concentration of H_2SO_4 as shown in Fig. 6 because the acidic concentration was excessively added to the reactor and final pHs of all the leached solutions were kept at pH 1.0.

Fig. 6 presents the fractional conversion of praseodymium during the leaching. As shown in Fig. 6, Pr_6O_{11} existing in the REE slag was completely leached out to $Pr_2(SO_4)_3$ solution after 5 h under the condition of slurry density of 1.500 g slag/L, 0.3 mol/L H_2SO_4 at 80 °C. During the leaching, the praseodymium concentrations were analyzed by ICP-AES. Initial leaching reaction was fast accomplished within 20 min or below as soon as raw material poured into the reactor. After that time, the leaching rate rapidly decreased. Therefore, this leaching reaction was suggested as a two-step model.

The conversion rate of REE slag could be divided into two stages on the basis of reaction time of 20 min: a rapid chemical reaction and a slow reaction stage.

Particle size of slag raw material had a range of 100-200 μm and it kept the same size approximately after the leaching reaction as shown in Fig. 7. From the result, we could know that the slag has
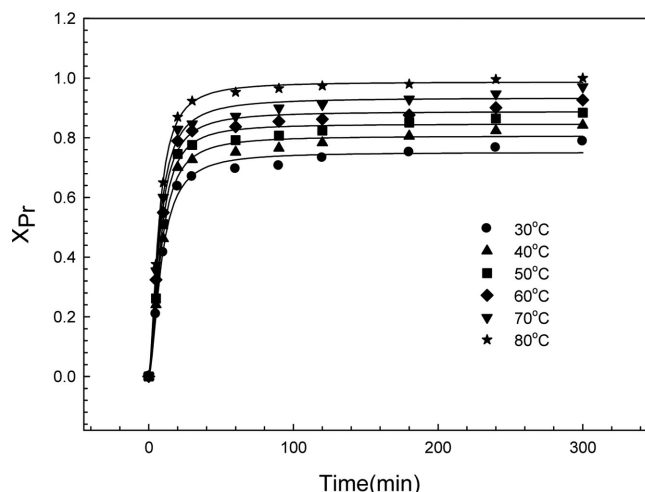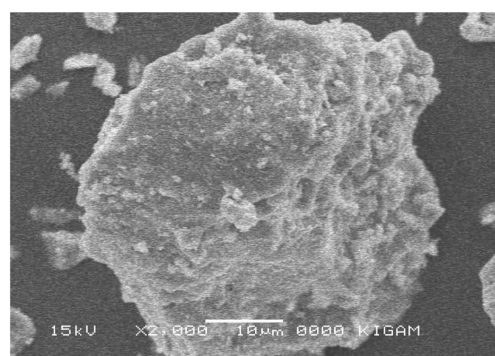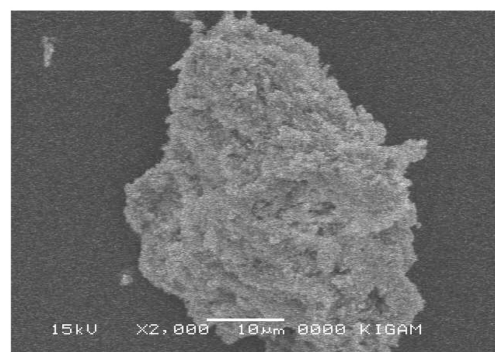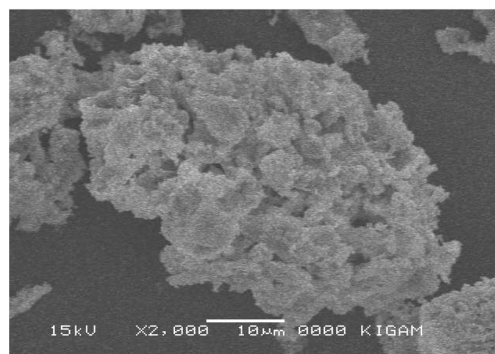

Fig. 6. Evolution of praseodymium fractional conversion.

(a)

(b)

(c)

Fig. 7. SEM photographs of slag at leaching times: (a) 0 min (b) 30 min, and (c) 300 min.

unreacted layers and these layers act as a resistance over leaching reaction. The reaction introduced a shrinking core model with a constant particle size. Reaction rate was measured by the analysis of praseodymium concentration by ICP-AES.

In the experiment it was assumed that there was no change of concentration during the leaching reaction because the H_2SO_4 was excessively added than the stoichiometric ratio necessary in the reaction. This experiment was fixed at the condition of 0.3 mol/L H_2SO_4 concentration to neglect the change of H_2SO_4 concentration during the leaching. As described before, the chemical species stable in the solution was determined by $Pr_2(SO_4)_3$ solution phase because the final leached solution indicated the scale of pH 1.0.

4-1. Chemical reaction control

If REEs included in the slag exist as a form of oxide, the stoichiometric ratio of H_2SO_4 based on the result of ICP-MS is 0.018 mol H_2SO_4 per 1.500 g. In the present experiment, H_2SO_4 was added 0.3 mol over the stoichiometric ratio. Therefore, it can be assumed that C_A is constant during the leaching.

The rate equation can be summarized as in Eq. (5) using the shrinking core model [20,21] that has the shape of a spherical particle. On the basis of Eq. (5), the apparent rate constant ($k_{c,chem}$) can be calculated by the least square method at reaction temperatures as shown in Fig. 8.

Table 2 shows kinetic constants ($k_{c,chem}$) at the chemical reaction stage calculated by the least square method from the slopes of each graphs in Fig. 8.

To examine the effect of reaction temperatures, the apparent activation energy was calculated from rate constants according to the temperatures as shown in Table 2. In the case of the chemical reac-
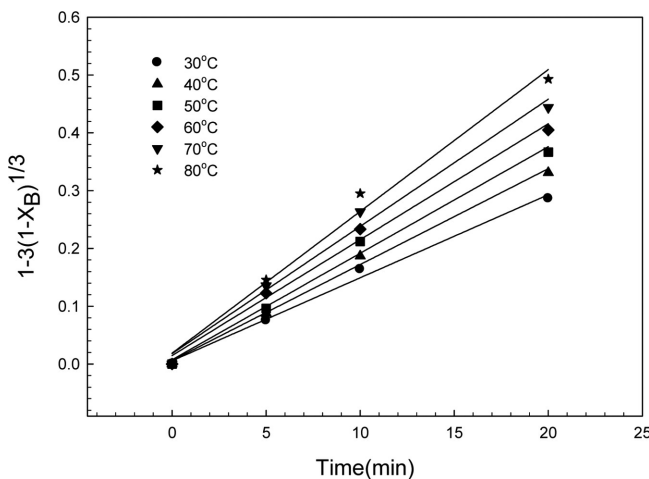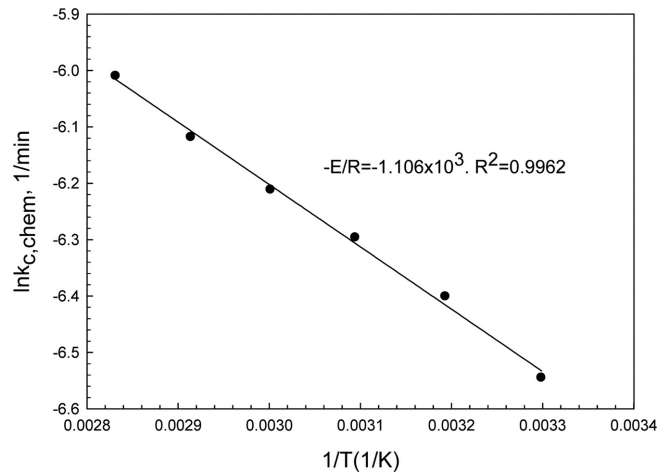

Fig. 9. Arrhenius plot of chemical reaction stage.

tion control, the apparent activation energy was calculated at 9.195 kJmol^{-1} from the slope of the graph in the range of 30 to 80 °C as shown in Fig. 9.

4-2. Ash layer diffusion

Chemical reaction is a rate determining step before 20 min. However, as shown in Fig. 8, REE components on the surface the slag are reacted with H_2SO_4 and leached out by chemical reaction. After all the slag surface becomes rough and remains only ash layer after REE leaching. The ash layer will act as a resistance for H_2SO_4 to go into inner layer to be REE components. Accordingly, the ash layer diffusion was assumed as a second stage after a chemical reaction.

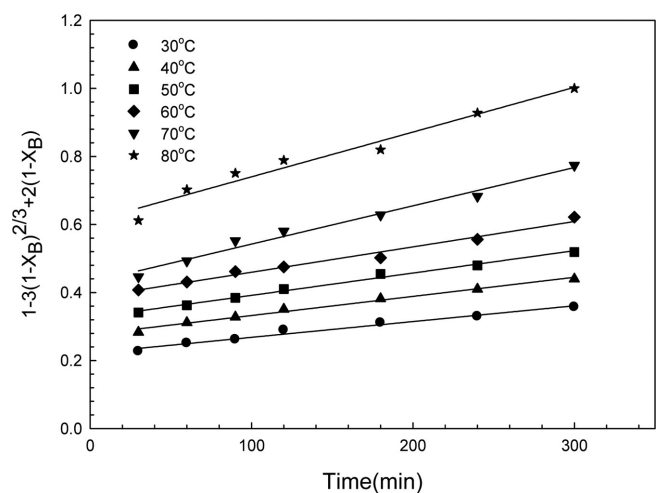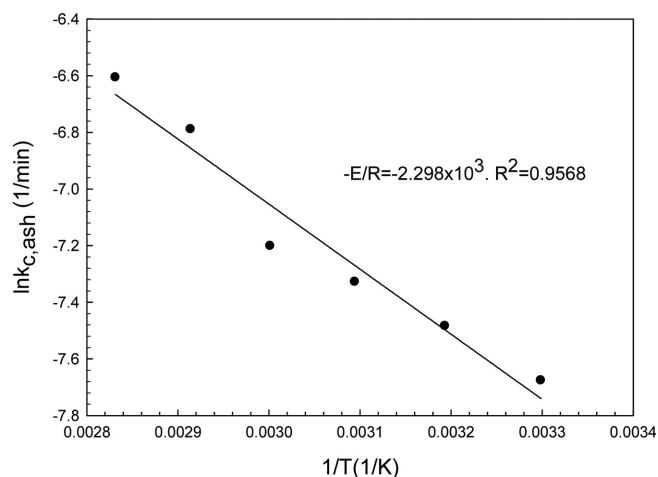The rate equation can be summarized as in Eq. (7) for ash layer

Fig. 8. Relationship between $1-3(1-X_B)^{1/3}$ and reaction time during chemical reaction stage.

Fig. 10. Relationship between $1-3(1-X_B)^{2/3}+2(1-X_B)$ and reaction time during ash layer diffusion stage.

Table 2. Parameter searching data obtained from the regression by $y = ax+b$ for chemical reaction determining step

Parameter	30 °C	40 °C	50 °C	60 °C	70 °C	80 °C
a	1.437×10^{-2}	1.660×10^{-2}	1.843×10^{-2}	2.006×10^{-2}	2.202×10^{-2}	2.454×10^{-2}
b	5.582×10^{-3}	6.184×10^{-3}	7.414×10^{-3}	1.468×10^{-2}	1.805×10^{-2}	1.873×10^{-3}
R^2	0.9936	0.9950	0.9925	0.9919	0.9886	0.9879

Table 3. Parameter searching data obtained from the regression by y=ax+b for ash layer diffusion determining step

Parameter	30 °C	40 °C		50 °C		60 °C
a	4.635×10^{-4}	5.618×10^{-4}	6.566×10^{-4}	7.452×10^{-3}	1.125×10^{-3}	1.351×10^{-3}
b	2.219×10^{-1}	2.762×10^{-1}	3.259×10^{-1}	3.851×10^{-1}	4.298×10^{-1}	6.086×10^{-1}
R^2	0.9780	0.9892	0.9923	0.9816	0.9819	0.9688

Fig. 11. Arrhenius plot of ash layer diffusion stage.

diffusion rate determining step using the shrinking core model that has the shape of a spherical particle. On the basis of Eq. (7), the apparent rate constant ($k_{c,ash}$) can be calculated by the least square method at various reaction temperatures as shown in Fig. 10.

Table 3 shows kinetic constants ($k_{c,ash}$) of the ash layer diffusion stage calculated by the least square method from the slopes of Fig. 10.

To examine the effect of reaction temperatures, the apparent activation energy was calculated from rate constants according to the temperatures as shown in Table 3. In the case of the ash layer diffusion control, the apparent activation energy was calculated at 19.106 kJmo^{-1} from the slope of the graph in the range of 30 to 80 °C as shown in Fig. 11.

5. Conclusions

The leaching mechanism of praseodymium in the H_2SO_4 from REE slag was proposed by a two-stage shrinking core model as the leaching rate determining stages, chemical reaction and ash layer diffusion.

Leaching efficiency of pure praseodymium oxide in acidic condition generally decreases with increasing temperatures, but this REE slag was oppositely increased because ash layer included in the slag acted a resistance against the leaching and the increase of temperature brings active molecular motion of H_2SO_4. In this experiment, the REE leaching could attain a 100% yield after the leaching of 5 h, 80 °C.

From the result of kinetic study, the first reaction was determined by rapid chemical reaction stage and the next reaction was determined by ash layer diffusion stage as the following results:

(1) In the initial chemical reaction control stage, leaching kinetics followed a shrinking core model with chemical reaction as the first rate-controlling step. The initial chemical reaction was completed within 20 min or below. The reaction rate and yield were increased according to the increase of temperature during the reaction. In the initial chemical reaction control stage, the activation energy was found to be 9.195 kJmol^{-1} between 30 and 80 °C. The postulated reaction was well confirmed by both the linear relationship of the rate constant and the apparent activation energy.

(2) Irrespective of initial rapid chemical reaction, the ash layer diffusion rate slowly proceeded because the ash layer acted as a resistance to block penetration of H_2SO_4. In the second ash layer diffusion stage, the apparent activation energy was determined by 19.106 kJmol^{-1} higher than the chemical reaction stage. Temperature dependence in the ash layer diffusion was relatively more temperature-sensitive than the chemical reaction control stage.

(3) Optimum condition for the recovery of praseodymium from the REE slag was given to the condition of slurry density of 1.500 g/L, 0.3 mol/L H_2SO_4, temperature of 80 °C, leaching time of 5 h. The leaching yield was proportional to the leaching temperature under the condition of excess H_2SO_4 over the stoichiometric ratio.

(4) In general, in the case of pure REEs, the more leaching temperature increases, the less solubility decreases, but the REE slag showed an opposite result because unreacted ash layer included in the slag acted as a resistance against the leaching.

In conclusion, the leaching rate and yield are proportional to the leaching temperature in the case of low-grade raw materials with unreacted ash layers.

Nomenclature

C_A : concentration of slag reactant (molL^{-1})
C_A : concentration of H_2SO_4 reactant (molL^{-1})
C_{A0} : initial concentration of H_2SO_4 reactant (molL^{-1})
C_B : concentration of REE slag reactant (molL^{-1})
C_{B0} : initial concentration of REE slag reactant (molL^{-1})
E_{Chem} : apparent activation energy for chemical reaction (kJmol^{-1})
E_{Ash} : apparent activation energy for ash layer diffusion (kJmol^{-1})
k_s : first-order rate constant for the chemical reaction (s^{-1})
$k_{c,chem}$: apparent rate constant for chemical reaction (s^{-1})
$k_{c,ash}$: apparent rate constant for ash layer diffusion (s^{-1})
N_A : moles of H_2SO_4 reactant (mol)
N_B : moles of REE slag reactant (mol)
N_{B0} : initial moles of REE slag reactant (mol)
r_c : radius of unreacted slag (m)

R   : radius of initial slag (m)
S_{ex} : external surface area (m^2)
t   : time (s)
T   : temperature (K)
X_A : fraction of converted H$_2$SO$_4$
X_B : fraction of converted praceodymium in REE slag

Greek Letter

ρ_B : molar density of praseodymium component included in slag (molL^{-1})

Acknowledgments

References

1. IUPAC, *Nomenclature of Inorganic Chemistry*, IUPAC Recommendations 2005("Red book"), RSC Publishing, Cambridge (UK), ISBN: 0-85404-438-8(2005).
2. Antolini, E. and Perez, J., "The Use of Rare Earth-based Materials in Low-temperature Fuel Cells," *Int. J. Hydrog. Energy*, **36**, 15752-15765(2011).
3. Yu, Z. and Chen, M., *Rare Earth Elements and Their Applications*, Metallurgical Industry Press(1995).
4. Massari, S. and Ruberti, M., "Rare Earth Elements as Critical Raw Materials: Focus on International Markets and Future Strategies," *Resources Policy*, **38**, 36-43(2013).
5. Aarabi-Karasgani, M., Rashchi, F., Mostoufi, N. and Vahidi, E., "Leaching of Vanadium from LD Converter Slag Using Sulfuric Acid," *Hydrometallurgy*, **102**, 14-21(2010).
6. Dehghan, R., Noaparast, M. and Kolahdoozan, M., "Leaching and Kinetic Modelling of Low-grade Calcareous Sphalerite in Acidic Ferric Chloride Solution," *Hydrometallurgy*, **96**, 275-282(2009).
7. El-Nadi, Y. A., "Lanthanum and Neodymium from Egyptian Monazite: Synergistic Extractive Separation Using Organophosphorus Reagents," *Hydrometallurgy*, **119-120**, 23-29(2012).
8. Kim, C.-J., Yoon, H.-S., Chung, K. W., Lee, J.-Y., Kim, S.-D., Shin, S. M., Lee, S.-J., Joe, A.-R., Lee, S.-I., Yoo, S.-J. and Kim, S.-H., "Leaching Kinetics of Lanthanum in Sulfuric Acid from Rare Earth Element (REE) Slag," *Hydrometallurgy*, **146**, 133-137 (2014).
9. Kim C.-J., Yoon H,-S,, Chung K.W., Lee J.-Y., Kim S.-D., Shin S. M., Lee S.-J., Joe A.-R., Lee S.-I., Yoo S.-J. and Kim J.-G., "Leaching Kinetics of Neodymium in Sulfuric Acid from E-scrap of NdFeB Permanent Magnet," *Korean J. Chem. Eng.*, **31**, 706-711(2014).
10. Kostova, I., "Lanthanides as Anticancer Agents," *Curr. Med. Chem.*, **5**, 591-602(2005).
11. Kul, M., Topkaya, Y. and Karakaya, I., "Rare Earth Double Sulfates from Pre-concentrated Bastnasite," *Hydrometallurgy*, **93**, 129-135 (2008).
12. Liu, K., Chen, Q., Yin, Z., Hu, H. and Ding, Z., "Kinetics of Leaching of a Chinese Laterite Containing Maghemite and Magnetite in Sulfuric Acid Solutions," *Hydrometallurgy*, **125-126**, 125-136(2012).
13. Manhique, A. J., Focke, W. W. and Carvalho, M., "Titania Recovery from Low-grage Titanoferrous Minerals," *Hydrometallurgy*, **109**, 230-236(2011).
14. Minting, L., Chang, W., Shuang, Q., Xuejiao, Z., Cunxiong, L. and Zhigan, D., "Kinetics of Vanadium Dissolution from Black Shale in Pressure Acid Leaching," *Hydrometallurgy*, **104**, 193-200(2010).
15. Moldoveanu, G. A. and Papangelakis, V. G., "Recovery of Rare Earth Elements Adsorbed on Clay Minerals: I. Desorption Mechanism," *Hydrometallurgy*, **117-118**, 71-78(2012).
16. Yoo, S.-J., Yoon, H.-S., Jang, H. D., Lee, M.-J., Lee, S.-I., Park, S.-T. and Hong, H. S., "Dissolution Kinetics of Aluminum Can in Isopropyl Alcohol for Aluminum Isopropoxide," *Chem. Eng. J.*, **133**, 79-84(2007).
17. Yoo, S.-J., Kwak, D.-H., Lee, J.-W., Hwang, U.-Y. and Jang, H.-D., "Kinetics of Aluminum Can Dissolution in Sec-butyl Alcohol for Aluminum Sec-butoxide," *Hydrometallurgy*, **96**, 223-229(2009).
18. Levenspiel, O., *Chemical Reaction Engineering*, 3rd ed., Wiley, New York(1999).
19. Schmidt, L.D., *The Engineering of Chemical Reactions*, 2nd ed., Oxford University Press(2005).
20. Dickinson, C. F. and Heal, G. R., "Solid-liquid Diffusion Controlled Rate Equations," *Thermochim. Acta*, **340-341**, 89-103(1999).
21. Órfão, J. J. M. and Martins, F. G., "Kinetic Analysis of Thermogravimetric Data Obtained Under Linear Temperature Programming-a Method Based on Calculations of the Temperature Integral by Interpolation," *Thermochim. Acta*, **390**, 195-211(2002).
22. Akinlua, T. N. and Ajayi, T. R., "Determination of Rare Earth Elements in Niger Delta Crude Oils by Imductively Coupled Plasma-mass Spectrometry," *Fuel*, **87**, 1469-1477(2008).
23. Lichtfouse, E. (ed.), *Organic Farming, Pest Control and Remediation of Soil Pollutants, Sustainable Agriculture Review 1*, Springer Science+Business Media B.V(2009).
24. Clavier, N., Podor, R. and Dacheux, N., "Crystal Chemistry of the Monazite Structure," *J. European Ceram. Soc.*, **31**, 941-976(2011).
25. HSC Chemistry 5.0 Chemical Reaction and Equilibrium Software with Extensive Thermochemical Database. Ver 5.11, Outokumpu Research, Finland.